

## Searches in CMS for new physics in final states with leptons and photons

---

**Małgorzata KAZANA\*** on behalf of the CMS Collaboration

*National Centre for Nuclear Research, NCBJ,  
Ludwika Pasteura 7, 02-093 Warsaw, Poland*

*E-mail: [malgorzata.kazana@cern.ch](mailto:malgorzata.kazana@cern.ch)*

The CMS experiment at the CERN LHC conducts extensive searches for *new physics* in which leptons and photons provide clear signatures. Many exotic possibilities beyond the Standard Model are under consideration, including new gauge bosons or resonances, leptoquarks, Higgs-like particles, extra dimensions, dark matter, and more. In this overview, the recently released results on such searches from the full LHC Run-2 (2016-2018) dataset at  $\sqrt{s} = 13$  TeV and an integrated luminosity up to  $138 \text{ fb}^{-1}$  are presented.

*The European Physical Society Conference on High Energy Physics (EPS-HEP2023)  
21-25 August 2023  
Hamburg, Germany*

---

\*Speaker

The searches for *new particles* are one of the main goals of the CMS [1] experiment. In 2023, CMS performed searches using the LHC data from Run 2 (2016–2018) corresponding to an integrated luminosity of up to  $\mathcal{L} = 138 \text{ fb}^{-1}$  from proton-proton collisions at LHC at a centre-of-mass energy of 13 TeV. Despite an intensive work, no sign of *new physics* has been found so far. Therefore, more advanced techniques are used and the previously unexplored signatures are studied. The distinctive signatures arise from the presence of leptons and photons in the final state, which allow to probe not only high mass particles but also allow to get a sensitivity to low mass new particles at GeV scale. In this overview, selected CMS results of searches with leptons and photons are presented.

## 1. Search for pair production of leptoquarks decaying to muons and bottom quarks

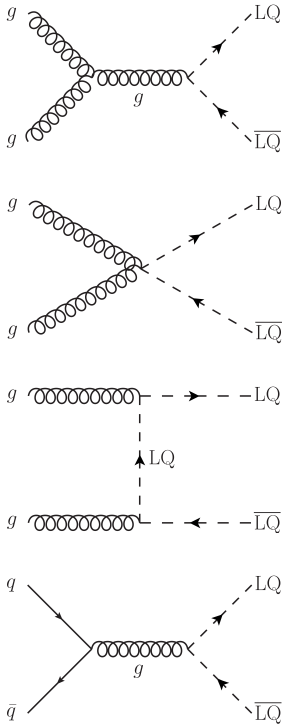


**Figure 1:** Feynman diagrams for a dominant leading-order pair production of scalar leptoquarks at the LHC. Ref. [2]

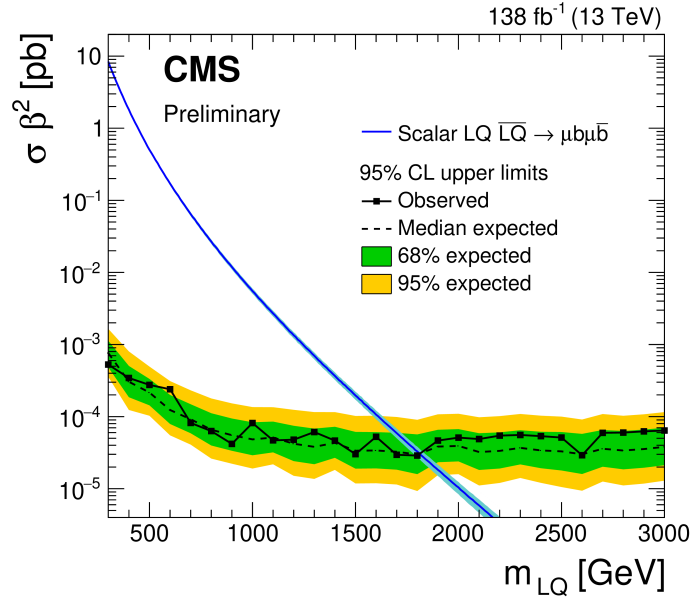


**Figure 2:** The expected and observed upper limits at 95% CL on the product of the scalar LQ pair production cross section and the branching fractions  $\beta^2$  as a function of the LQ mass,  $m_{LQ}$ . The solid line represents the observed limits, the dashed line represents the median expected limits, and the inner dark-green and outer light-yellow bands represent the 68% and 95% CL intervals. The blue curve with bands represents the theoretical production cross sections and its uncertainties. Ref. [2]

The leptoquarks (LQs) are hypothetical bosonic particles which can transform quarks to leptons and backwards. They have been searched for at CMS assuming that they couple to leptons and quarks of the same generation of matter, since it is motivated by experimental limits on processes like proton decay. However, recent measurements of the muon magnetic dipole moment from the Muon  $g-2$  experiment and earlier measurements of flavor anomalies from Belle and LHCb experiments, which have shown some inconsistencies with their SM predictions, motivated to introduce LQs

that couple to muons and quarks of a different generation (such as bottom quarks) to explain such discrepancies.

At the LHC, LQs may be produced alone or in pairs. The new CMS search [2] focuses on the production of pair of LQ and anti-LQ, as shown in the Feynman diagrams of Fig. 1 with each LQ decaying to a muon and a bottom (b) quark. The b quark hadronizes into a jet of particles in the detector and it is identified as a b-jet by an advanced deep learning algorithm [3] by using low-level features of the particle constituents inside the jet. In order to distinguish a possible LQ signal from background processes, multivariate machine learning techniques are used. A boosted decision tree (BDT) classifier is trained on background and signal for various LQ mass hypotheses.

Using all the data recorded by the CMS detector during the LHC Run 2 ( $\mathcal{L} = 138 \text{ fb}^{-1}$ ), no significant excess above the predicted background is identified for any LQ mass hypothesis. Limits are then set on the LQ pair production cross section as a function of LQ mass as shown in Fig. 2. By comparing the observed upper limit with values expected from theoretical models, leptoquarks decaying only to muon-bottom-quark pairs with a mass below 1810 GeV are excluded at 95 % confidence level (CL). These are the most stringent limits to date on LQ decaying to leptons and quarks from on the same generation.

## 2. Search for a high-mass dimuon resonance in association with b quark jets

Many theoretical models that aim to extend the SM predict the existence of a new heavy, neutral boson ( $Z'$ ) decaying to leptons ( $\ell$ ) with similar properties with regards to the SM Z boson. Among these models, scenarios where the new  $Z'$  interacts with bottom (b) and strange (s) quarks (like those depicted in Fig. 3) are of particular interest because the existence of such a  $Z'$  boson may have implications in low-energy  $b \rightarrow s\ell\ell$  interactions, which have been measured at the LHC [5, 6] and might be interpreted as hints for the presence of physics beyond the standard model (BSM).

A  $Z'$  boson produced in association with at least one b quark and decaying into a pair of oppositely-charged muons would leave a unique signature [4] in the CMS detector in the reconstructed dimuon invariant mass ( $m_{\mu\mu}$ ) distribution on top of the SM processes. The search adopted a strategy aimed at suppressing this source of background. The presence of the b-quark strongly disfavours Drell-Yan events. The  $m_{\mu\mu}$  obtained from the reconstructed top quark decay products has an endpoint at the top quark mass value, which can be used to veto  $t\bar{t}$  events.

The residual SM background contribution was estimated directly in data, by fitting the reconstructed dimuon invariant mass distribution in regions centered around the signal  $Z'$  mass hypothesis

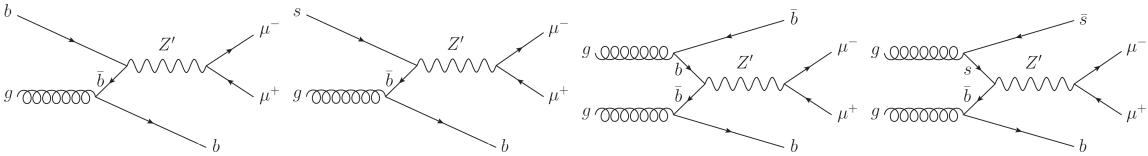


**Figure 3:** Feynman diagrams of  $Z' \rightarrow \mu^- \mu^+$  with a  $Z'$  boson produced via  $b\bar{b} \rightarrow Z'$  or  $s\bar{b} \rightarrow Z'$ , with at least one b quark in the final state. A coupling of  $Z'bb$  may be present in any generic model, but a  $Z'sb$  coupling could arise through flavor mixing between the second- and third-generation quarks. Ref. [4]

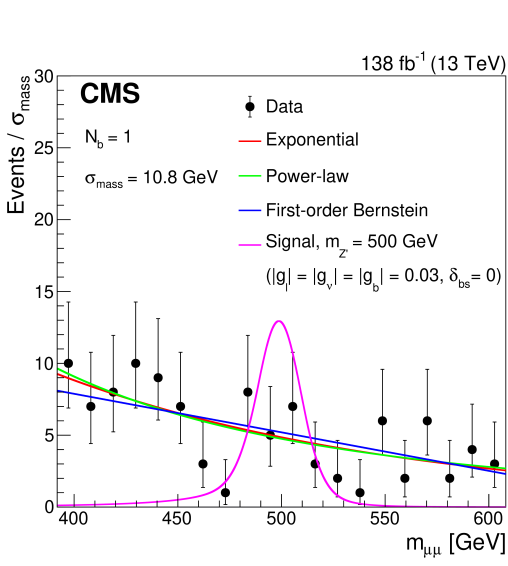


**Figure 4:** Dimuon invariant mass ( $m_{\mu\mu}$ ) distributions in events with one b quark jet. The  $m_{\mu\mu}$  distribution as obtained in data (black circles) is shown together with the functional forms used to fit the SM background, and the distribution expected for an hypothetical signal (magenta curve)  $Z'$  with a mass of 500 GeV. Ref. [4]

being probed. The signal, if present, would have appeared as a narrow bump at the center of the window, as shown in Fig. 4.

The limits are derived for  $\mathcal{L} = 138 \text{ fb}^{-1}$  on the total number of signal events with  $N_b = 1$  and  $\geq 2$ , where  $N_b$  denotes the multiplicity of b quark jets, and these limits are model independent to the extent that the signal arises from the direct production and subsequent decay of a narrow dimuon resonance. The relative fraction of events with  $N_b \geq 2$  is varied to probe a range of hypotheses of signal production in association with b quarks. The limits are presented as a function of the analyzed dimuon resonance mass values, as illustrated in Fig. 5.

Constraints are also set on a specific  $Z'$  model ( $B_3 - L_2$ ), constructed to accommodate possible contributions to  $b \rightarrow s\ell\ell$  transitions beyond the standard model. In this scenario, most of the allowed parameter space is excluded for a  $Z'$  boson with  $350 < m_{Z'} < 500$  GeV, while the constraints are less stringent for higher  $m_{Z'}$  hypotheses. This is the first dedicated search at the LHC for a high-mass, narrow dimuon resonance produced in association with multiple b quark jets, and the constraints obtained on models with this signature are the most stringent to date.

### 3. Search for resonances in multilepton final state in associated production

A search [7] for BSM scalar, pseudoscalar and Higgs-like bosons that decay into pairs of electrons, muons, or tau leptons is presented. The search probes new  $\phi$  bosons that are produced

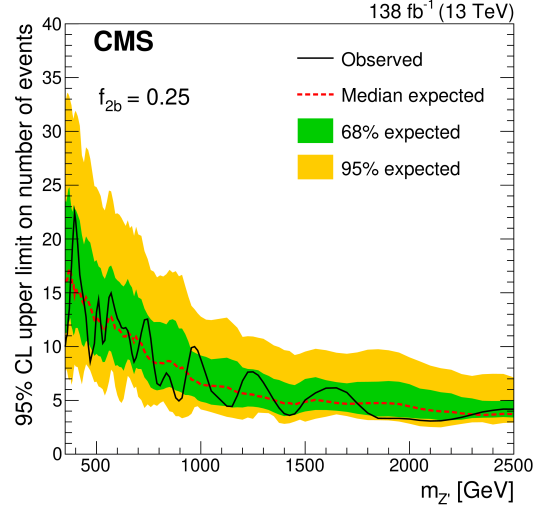


**Figure 5:** Exclusion limits at 95% CL on the number of selected BSM events with  $N_b \geq 1$  as functions of  $m_{Z'}$  for  $f_{2b} = 0.25$ , where the quantity  $f_{2b}$  is the fraction of BSM events passing the analysis selections that have  $N_b \geq 2$ . The solid black (dashed red) curve represents the observed (median expected) exclusion. The inner green (outer yellow) band indicates the region containing 68 (95)% of the distribution of limits expected under the background-only hypothesis. Ref. [4]

in association with a W or Z boson, or a top quark anti-top quark pair, in events with with three or four leptons, including hadronic decays of tau leptons, as depicted in Fig. 6.

Tight selection and isolation criteria are applied on electrons and muons, and tau decays are reconstructed in the hadronic channel. Events are categorized into tree or four lepton final states with all combination of leptons, giving 24 signal final state categories  $X\phi$ , where X is W or Z boson or the  $t\bar{t}$  pair.

The irreducible background as prompt and mis-identified leptons is estimated either from simulation or sidebands in data. The opposite-sign same-flavour (OSSF) dilepton mass is used as main discriminating variable, enabling sensitivity to low invariant masses. Finally, the  $\phi$  mass is probed in the mass range of 15-76 GeV and 106-366 GeV, to exclude the Z boson in range of the mass  $91 \pm 15$  GeV.

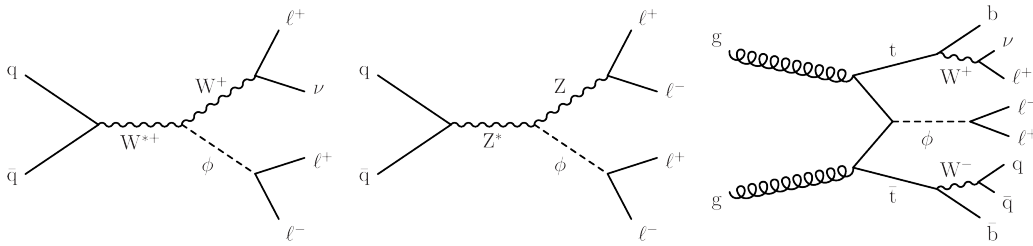


**Figure 6:** Example production and decay diagrams for dilepton resonance in associated production with  $W\phi$ ,  $Z\phi$ , and  $t\bar{t}\phi$ , producing multilepton final states. Ref. [7]

No statistically significant deviation from the SM expectations in any of the probed dilepton mass distributions is observed. The largest local deviation is observed in the high mass  $Z\phi \rightarrow ee$  search, as illustrated in Fig. 7, where one can observe an excess at the dielectron mass of 156 GeV corresponding to 2.9 standard deviations ( $\sigma$ ) locally and 1.4  $\sigma$  globally. All other excesses or deficits in all other production, coupling, and decay scenarios are less significant.

Upper limits at 95% CL for the full Run 2 data set ( $\mathcal{L} = 138 \text{ fb}^{-1}$ ) are placed on the product of cross section and branching fraction of such new particles with scalar, pseudoscalar, or Higgs-like couplings. Considering a single production, coupling, and decay scenario at a time, the observations exclude product of cross section and branching fraction values above a range of 50 fb and 0.5 fb for new scalar, 30 fb and 0.5 fb for new pseudoscalar and 200 fb and 1 fb for new Higgs-like bosons, that have a mass in the range 15-350 GeV and exclusively decay into dielectron or dimuon pairs, as illustrated in one of set of limits in Fig. 8. Similarly, assuming such new bosons exclusively decay into pairs of tau leptons, the product of cross section and branching fraction values above ranges of 35 pb and 4 fb, 80 pb and 4 fb, and 250 pb and 8 fb are excluded for scalar, pseudoscalar, and Higgs-like couplings, respectively. These are the most restrictive direct limits in these production and decay modes on an extension of the standard model with scalar or pseudoscalar particles.

#### 4. Search for resonances in events with photon and jet final states

The CMS Collaboration has performed a search for resonances in events with a photon plus jet final state [8]. Models of excited quarks and quantum black holes (QBH) shown in Fig. 9 are considered. The invariant mass spectrum of the  $\gamma+$  jet system is examined for the presence

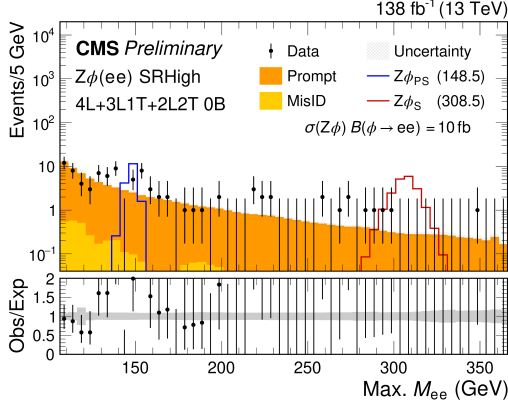


**Figure 7:** Dilepton mass spectra for the  $Z\phi(ee)$  signal region for high mass selections for the combined 2016-2018 data set. The lower panel shows the ratio of observed events to the total expected SM background prediction, and the gray band represents the sum of statistical and systematic uncertainties in the background prediction. The expected background distributions and the uncertainties are shown after fitting the data under the background-only hypothesis. For illustration, two example signal hypotheses for the production and decay of a scalar ( $\phi_S$ ) and a pseudoscalar ( $\phi_{PS}$ ) boson are shown. Ref. [7]

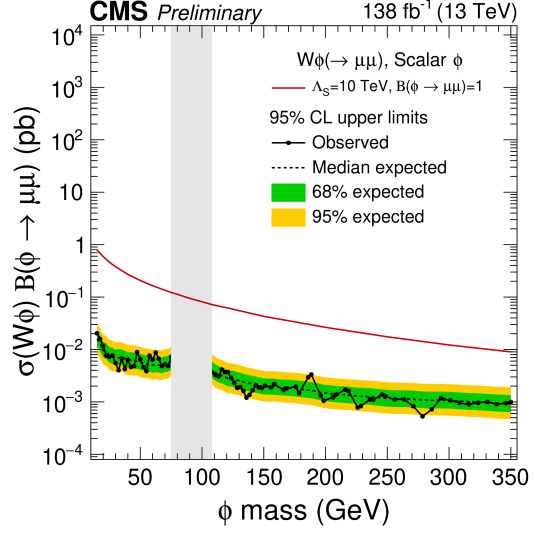


**Figure 8:** The 95% confidence level upper limits on the product of the signal production cross section and branching fraction of the  $W\phi$  signal model where the  $\phi$  boson has a scalar coupling. The vertical gray band indicates the mass region not considered in the analysis. The red line is the theoretical prediction for the product of the production cross section and branching fraction of the  $W\phi$  model. Ref. [7]

of resonances over the standard model continuum background. Events are selected if they have a high transverse momentum photon ( $p_T > 240$  GeV and  $|\eta| < 1.4$ ) and a wide-jet ( $p_T > 170$  GeV and  $|\eta| < 2.4$ ) combining within a wide cone of  $\Delta R < 1.1$  narrow jets ( $p_T > 30$  GeV and  $|\eta| < 3$ ) with a cone size of  $\Delta R < 0.4$ . Additionally, a b-tagging of jet is required for the excited bottom quark search. The main discriminating variable is the invariant mass ( $m_{\gamma+jet}$ ) of the highest- $p_T$  photon and the highest- $p_T$  jet for  $\Delta R(\gamma, \text{wide-jet}) > 1.1$  and  $\Delta\eta(\gamma, \text{wide-jet}) < 1.5$ .

The main background to this analysis are  $\gamma + jet$  production, quantum chromodynamics (QCD) multijet production, and  $W/Z + \gamma$  processes. The background is estimated directly from data by fitting the mass distribution with a polynomial fit. Results are presented in Fig. 10. The data from the full Run 2 ( $\mathcal{L} = 138 \text{ fb}^{-1}$ ) exhibit no statistically significant deviations from the expected standard model background. Therefore, the exclusion limits at 95% CL on the resonance mass and other parameters are set and plotted in Fig. 11. Excited light-flavor quarks (excited bottom quarks) are excluded up to a mass of 6.0 (3.8) TeV.

The quantum black hole production is excluded for masses up to 7.5 (5.2) TeV in the Arkani-Hamed–Dimopoulos–Dvali, ADD (Randall–Sundrum, RS) model as follows from exclusion limits shown in Fig. 12. These lower mass bounds are the most stringent to date among those obtained in the  $\gamma + jet$  final state.

## 5. Search for high-mass exclusive diphoton production with tagged protons

The CMS and TOTEM collaborations have performed a search [9] for high-mass exclusive diphoton production via photon-photon fusion in proton-proton collisions at  $\sqrt{s} = 13$  TeV in events where both protons survive the interaction. The process of exclusive production of two photons in photon fusion is usually called light-by-light (LbL) scattering has already been observed by ATLAS and CMS in electromagnetic ultraperipheral collisions (UPCs) of heavy ions, as illustrated in Fig. 13. Proton-proton collisions, on the other hand, feature higher beam energies and luminosities, and harder photon spectra than heavy ion UPCs. By tagging the surviving final state protons, one can better identify the process and study four-photon anomalous quartic gauge couplings (aQGC) at the multi-TeV scale. The LbL scattering allows probing of multiple BSM phenomena including the production of axion-like particles (ALP).

The analysis utilizes data corresponding to an integrated luminosity of  $103 \text{ fb}^{-1}$  collected in 2016-2018 with the central CMS detector and the CMS and TOTEM precision proton spectrometer (PPS). The PPS detector consists from Roman Pots and timing detectors, and it is located symmetrically (as a positive and negative arms) in a distance of 210-220 meters on both sides of the CMS detector.

The LbL signal events are selected by requiring the measurement of two high- $p_T$  photons emitted back-to-back, in coincidence with two opposite-side forward protons, measured in PPS, whose kinematic properties match those of the central diphoton system. The matching of two measurements from CMS and PPS detectors is illustrated in Fig. 14. The data are found to be in agreement with the predicted SM background, with 1 event observed and  $1.10 \pm 0.00$  (stat)  $\pm 0.24$  (syst) events expected. An upper limit on the LbL cross section of  $\sigma(pp \rightarrow p\gamma\gamma p) < 0.61 \text{ fb}$  is set within the fiducial range of the analysis defined as  $p_T^\gamma > 100 \text{ GeV}$ ,  $|\eta^\gamma| < 2.5$ ,  $m_{\gamma\gamma} > 350 \text{ GeV}$ , and fractional proton energy loss of  $0.035 < \zeta_p < 0.150(0.180)$  for the positive-z (negative-z) arm of PPS.

Limits at 95 % CL are derived for the  $4\gamma$  anomalous quartic gauge coupling parameters  $|\xi_1| < 0.073 \text{ TeV}^{-4}$  and  $|\xi_2| < 0.15 \text{ TeV}^{-4}$  (setting, alternatively, the other to zero), using an effective field theory and shown in Fig. 15.

Additionally, limits on the production of axion-like particles coupling to photons with strengths  $f^{-1} \approx 0.03$  to  $1 \text{ TeV}^{-1}$  are set over the mass range from 500 to 2000 GeV, as shown in Fig. 16. These are the most restrictive limits to date on  $4\gamma$  aQGC and on ALPs coupling to photons, in the very high mass phase space region.

## 6. Summary and prospects

The CMS experiment has built up a rich program [10] of *new physics* searches where SM leptons and photons provide exceptionally clear signatures. A large set of signatures is studied including searches for leptoquarks, generic analyses with new resonances, signals with heavy flavours, probing low mass exotic bosons or studying distinctive signature of light-by-light scattering. Since no signal of new particles is found with the full Run 2 LHC data, limits are set progressively on more massive hypothetical particles and the sensitivity to test low mass hypothetical particles is also extended.

Further improvements are expected with more data from Run 3 and newer techniques of machine learning.

## References

- [1] CMS Collaboration, "The CMS experiment at the CERN LHC", JINST **3**,S08004 (2008).
- [2] CMS Collaboration, "A search for pair production of leptoquarks decaying to muons and bottom quarks at  $\sqrt{s} = 13$  TeV". CMS-EXO-21-019.
- [3] Bols, E. and Kieseler, J. and Verzetti, M. and Stoye, M. and Stakia, A., "Jet flavour classification using DeepJet". JINST **15** (2020) P12012, arXiv:2008.10519 .
- [4] CMS Collaboration, "Search for a high-mass dimuon resonance produced in association with b quark jets at  $\sqrt{s} = 13$  TeV". JHEP **10** (2023) 043, arXiv:2307.08708.
- [5] LHCb Collaboration, "Angular analysis of the  $B^0 \rightarrow K^{*0} \mu^+ \mu^-$  decay using  $3 \text{ fb}^{-1}$  of integrated luminosity". JHEP **02** (2016) 104, arXiv:1512.04442.
- [6] CMS Collaboration, "Measurement of angular parameters from the decay  $B^0 \rightarrow K^{*0} \mu^+ \mu^-$  in proton-proton collisions at  $\sqrt{s} = 8$  TeV". Phys. Lett. B **781** (2018) 517, arXiv:1710.02846.
- [7] CMS Collaboration, "Search for dilepton resonances from decays of (pseudo) scalar bosons produced in association with a massive vector boson or top quark-antiquark pair in proton-proton collisions at  $\sqrt{s} = 13$  TeV". CMS-EXO-21-018.
- [8] CMS Collaboration, "Search for resonances in events with photon and jet final states in proton-proton collisions at  $\sqrt{s} = 13$  TeV". CMS-EXO-20-012, arXiv:2305.07998.
- [9] CMS and TOTEM Collaboration, "Search for high-mass exclusive diphoton production with tagged protons in proton-proton collisions at  $\sqrt{s} = 13$  TeV". CMS-EXO-21-007, arXiv:2311.02725, submitted to Phys. Rev. D.
- [10] <https://cms-results.web.cern.ch/cms-results/public-results/preliminary-results/EXO/index.html>

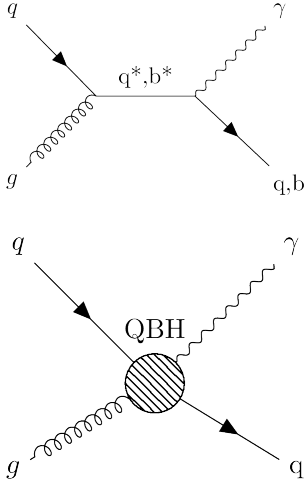


**Figure 9:** Illustrative Feynman diagrams for  $qg \rightarrow \gamma + \text{jet}$  resonance signal models of  $q^*$ ,  $b^*$  and the quantum black hole production. Ref. [8]

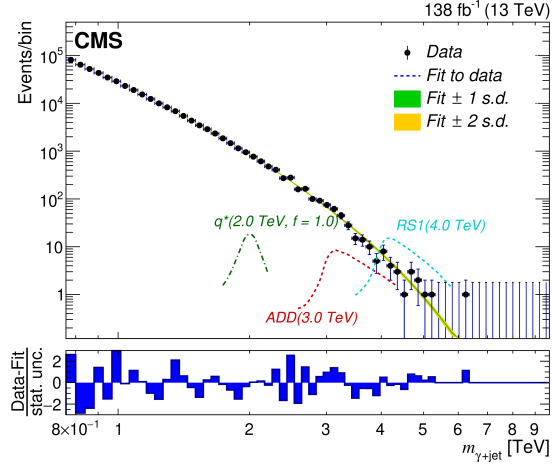


**Figure 10:** Fit to the  $\gamma + \text{jet}$  invariant mass distribution in data for the *inclusive* category of  $q^*$  and QBH after all selections. The green (inner) and yellow (outer) bands, respectively, represent the 68 and 95 % CL statistical uncertainties in the fit. Simulations of the  $q^*$ , ADD and RS1 signal are also shown. The lower panel shows the difference between the data yield and the background prediction divided by the statistical uncertainty of the data. Ref. [8]

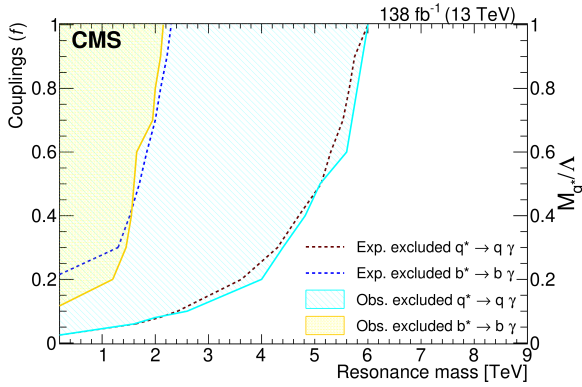


**Figure 11:** The expected and observed 95 % CL exclusion mass limit variation with the SM couplings for the excited  $q^*$  and  $b^*$  signal models. Ref. [8]

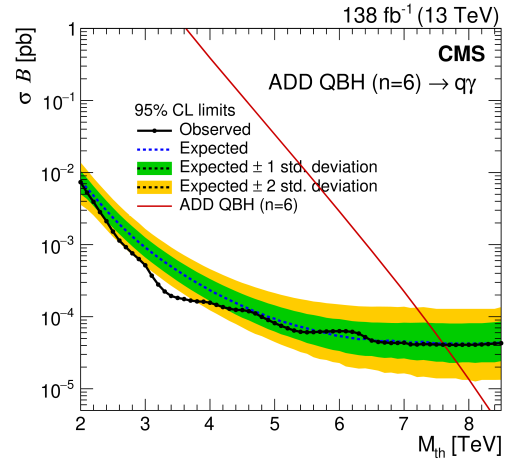


**Figure 12:** The expected (dashed) and observed (solid) 95 % CL upper limit on the product of the cross section and branching fraction as a function of the minimum black hole mass for the ADD ( $n=6$ ) model. The green (inner) and yellow (outer) bands correspond to 1 and 2 standard deviation uncertainties in the expected limit. Ref. [8]

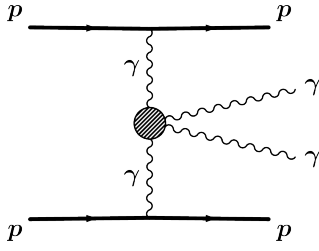


**Figure 13:** Diagram of LbL with intact protons in the final state. The four-photon vertex includes virtual contributions from SM or BSM charged fermions or bosons. In other BSM scenarios, a new heavy particle can be produced in the s-channel, such as an axion-like particle that decays into two photons. Ref. [9]

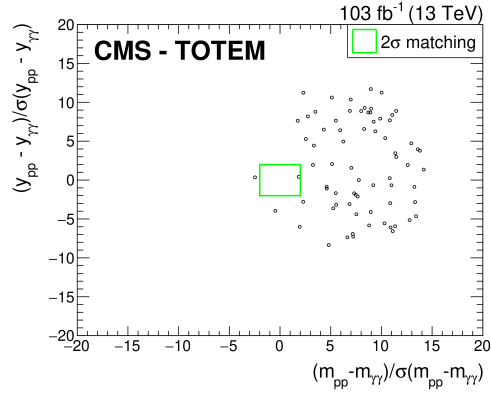


**Figure 14:** Mass versus rapidity matching distributions for events passing the selection criteria of diphoton detected in the CMS detector and diproton caught by the PPS TOTEM arm detectors. The matching (green) window of two standard deviations define a region where the signal is expected. Ref. [9]

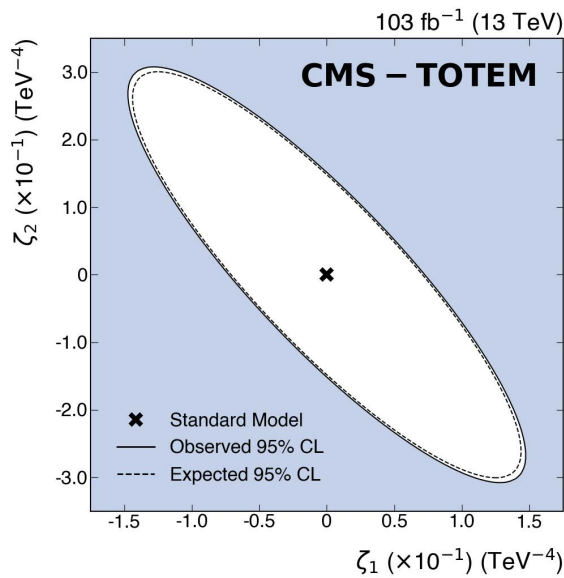


**Figure 15:** Observed (solid ellipse) and expected (dashed ellipse) exclusion limits at 95% CL on the anomalous coupling parameters  $\xi_1$  and  $\xi_2$  from the LbL search in pp collisions at 13 TeV. Ref. [9]

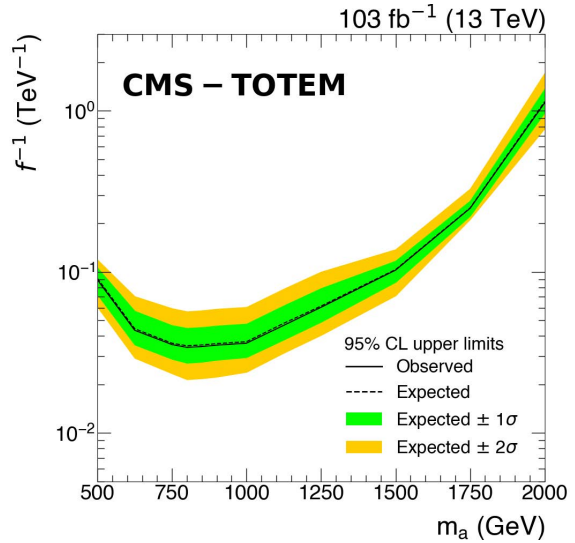


**Figure 16:** Upper limits at 95% CL on ALP-photon coupling strength as a function of the ALP mass. The shape of the limit curve is determined by the PPS efficiency-times-acceptance curve. The expected limits almost completely overlap with the observed ones. Ref. [9]